Dual-function circular polarization converter for microwave/plasma processing systems

T. H. Chang, L. R. Barnett, and K. R. Chu[a)]
Department of Physics, Nation Tsing Hua University, Hsinchu, Taiwan, Republic of China

F. Tai and C. L. Hsu
Chung-Shan Institute of Science and Technology, Lung-Tang, Taoyuan, Taiwan, Republic of China

Generation of a uniform density plasma has been a key consideration in the design of microwave/plasma processing systems. A circularly polarized wave can generate a plasma with good azimuthal uniformity as well as provide strong resonant interaction with the plasma electrons. In this article, we report the development of a three-port polarization converter which efficiently converts the TE_{10} wave of a standard rectangular waveguide into a circularly polarized TE_{11} wave of a cylindrical waveguide. Employing the same principle for mode conversion, the converter is also made to function as a protective device of the high power microwave source by providing a separate port for the return and damping of the reflected wave. Such a converter has been analyzed, constructed, and tested. At the operating frequency of 2.45 GHz, test results indicate a 25 dB return loss, 97% end-to-end polarization conversion efficiency, and better than 20 dB rejection of the reflected wave. The structural simplicity of the device allows high power operation as well as easy construction for system research and applications. © *1999 American Institute of Physics.*
[S0034-6748(99)01402-1]

I. INTRODUCTION

Design considerations for microwave/plasma processing systems are dictated by factors such as the gas pressure, ionization rate, plasma uniformity, ion energy, and etching/deposition efficiency.[1–5] Electron cyclotron resonance (ECR) heating[6–13] has been an actively researched as well as commercially employed method for plasma generation. Advantages of this method include low gas pressure, high fractional ionization, and low ion bombarding energies. In the ECR system, electrons are immersed in a region of magnetic field where the electron cyclotron frequency equals the wave frequency. A wave of arbitrary polarization launched into the interaction chamber can be viewed as the sum of two counter-rotating circularly polarized waves. The component which rotates in the same sense as electrons will resonantly interact with the electrons, resulting in a continuous gain of electron transverse energy. It is thus expected that a single resonant component of the circularly polarized wave will be most efficiently absorbed by the electrons.

Different ways have been considered to control the plasma uniformity in the ECR system. These generally involve a combination of optimized radio frequency (rf) field pattern, magnetic field profile, and chamber geometry.[2,3,14] The circularly polarized wave, with its axisymmetric power flow, will again be advantageous in generating an azimuthally uniform plasma.

There are various methods to obtain circular polarization. A common technique for producing circular polarized wave in the lowest order (TE_{11}) mode has been to split the input signal into two or four equal amplitude paths but 90° phase shifted (e.g., a turnstile junction)[9,15] which is then injected through apertures 90° apart around the circumference of the circular waveguide. Thus, there is the problem of obtaining the proper amplitude split and phase shift and maintaining it over the required bandwidth. Stevens *et al.* reported such a polarizer with 98% mode purity as well as rejection of the reflected wave.[9] Another commonly employed technique is implemented in a device known as the septum polarizer. This three port device consists of a square waveguide bifurcated by a notched or stepped septum into two standard rectangular waveguides, one as the input port and the other as the reflected wave port. By proper mode matching in the septum section, a TE_{10} wave launched into the input port will split into a TE_{10} mode and TE_{01} mode in the square output waveguide, equal in amplitude and 90° separated in phase. If the thickness of the septum is taken into consideration, it will be difficult to simultaneously control the relative amplitude and phase of the two waves. The design outlined above is generally useful for narrow bandwidth applications.[16,17] A recent study[18] shows that it is possible to obtain excellent bandwidth performance (up to 20%), low return loss, and high isolation by using ridged waveguides and a stepped-thickness septum.

Here, we consider a circular polarization converter based on a different principle. It features a single port for wave input and a separate port for the return and absorption of any wave that may be reflected from the plasma chamber. The main element of the converter consists simply of a straight circular waveguide with its middle section squeezed into slightly elliptical cross-section. A wave linearly polarized at 45° angle with respect to the major and minor axes, upon

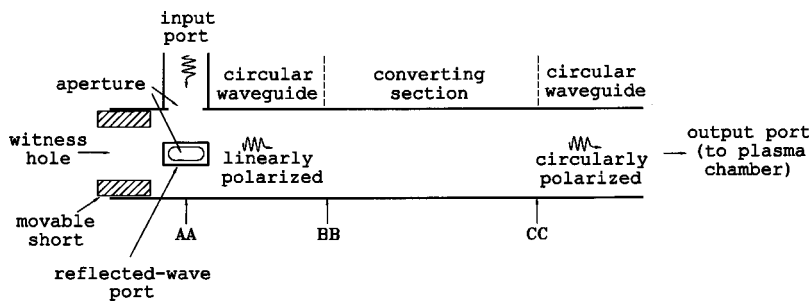[a)]Electronic mail: krchu@phys.nthu.edu.tw

FIG. 1. A schematic of the circular polarization converter. The converting section is a slightly flattened circular waveguide. Cross-sectional views at planes *AA*, *BB*, and *CC* are shown in Fig. 2.

entering the elliptical section, will split into two equal-amplitude waves linearly polarized along the major and minor axes, respectively, and propagating at different phase velocities.[19] The length of the elliptical section is chosen such that the accumulated phase angle difference will be 90°, thus allowing the two waves to combine into a circularly polarized wave when emerging from the other end of the elliptical converting section. Such a converter was originally developed in the *Ka* band and used successfully in our gyrotron traveling wave experiments.[20,21] Here we present the first documentation of its operating principles, structural details, and the test results of an *S*-band model intended for use in microwave/plasma processing system research.

Section II details the principle of mode conversion as well as the mechanism for the separation of the reflected wave from the input port. Construction and testing of a prototype model are presented in Sec. III.

II. PRINCIPLE OF OPERATION

Figure 1 illustrates the circular polarization converter under study. We divide the mode conversion processes into three stages and discuss below the operational principle involved in each stage.

A. Input coupling

A standard rectangular input waveguide operating in the fundamental (TE_{10}) mode is attached at right angle to the sidewall of a circular waveguide where an aperture couples the two waveguide sections. A microwave short is placed to the left of the aperture to cause all the microwave signal to propagate to the right. The microwave short is a circular tube with the inner diameter made small enough to completely attenuate the mode of interest and large enough to allow visual inspection of the plasma chamber downstream.

B. Conversion to circular polarization

As the linearly polarized TE_{11} wave propagates down the circular waveguide, it enters a radially perturbed converting section. The radial perturbation can be of a flattened circular shape as illustrated in Fig. 2(b) in which the axes denoted by r_1 and r_2 will be referred to as the minor and major axes, respectively. The two axes are tilted 45° with respect to polarization of the TE_{11} wave. This causes the TE_{11} wave to be split into two equal-amplitude linearly polarized TE_{11} waves with polarization being parallel to the major and minor axes [Fig. 2(c)]. Waves 1 and 2 will propagate at different phase velocities which are primarily deter-

mined by dimensions r_1 and r_2, respectively. When the two waves have propagated a distance sufficient to cause a 90° phase difference, the resultant sum of the two waves then becomes a circularly polarized wave [Fig. 2(d)]. At that point, the waveguide cross section is changed back into circular shape and the circularly polarized TE_{11} mode continues to propagate toward the plasma chamber.

C. Isolation of the reflected wave

When a reflection takes place downstream at the plasma chamber, due to the sudden formation of a plasma for example, the reflected wave will be circularly polarized just as the incident wave. However, as it propagates backward along the converting section, its two linearly polarized components will accumulate an additional 90° phase difference, resulting in a total phase difference of 180° as they emerge from the left end of the converting section. The sum then becomes a linearly polarized TE_{11} wave again, except that its polarization is now rotated by 90° with respect to that shown in Fig. 2(a). Hence the reflected wave will come out of the reflected-wave port which is made identical to the input port but located 90° apart [Fig. 2(a)]. Isolation of the reflected wave from the input port serves to protect the high power microwave source under mismatched conditions.

Since the input- and reflected-wave ports are identical, their functions can be interchanged. But then the output wave will be circularly polarized in the clockwise sense, i.e., opposite to that shown in Fig. 2(d).
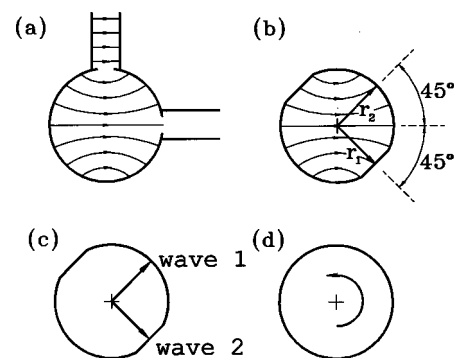

FIG. 2. Geometric shape and electric field pattern at different cross-sectional planes of the converter in Fig. 1 as viewed through the witness hole on the left. (a) Coupling of the rectangular TE_{10} mode to circular TE_{11} mode through the aperture at plane *AA*, (b) electric field pattern of the wave as it enters the converting section at plane *BB*, (c) splitting of the wave in (b) into two linearly polarized waves at plane *BB*, and (d) the circularly polarized wave as it emerges from the converting section at plane *CC*.
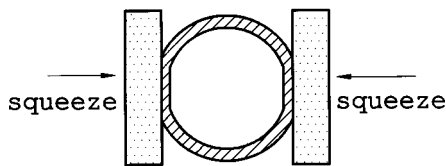
FIG. 3. Illustration of the squeezing technique for producing the radial perturbation on the converting section.

For the purpose of comparing the effects of linearly and circularly polarized waves on ECR plasma generation, the converter can be modified to generate a pure linearly polarized wave by simply removing its mode converting section.

III. CONSTRUCTION AND TESTING OF AN *S*-BAND POLARIZATION CONVERTER

The polarization converter shown in Fig. 1 can be constructed and optimized with simple tools and a modest amount of experimenting. The position of the microwave short and the size of the sidewall aperture are adjusted to provide efficient (nearly 100%) coupling of TE_{10} mode of the rectangular waveguide to the linearly polarized TE_{11} mode in the circular waveguide [Fig. 2(a)]. This is quite readily done when the operating frequency is below the cutoff frequencies of any high order modes in either waveguide. The reflected-wave port is made identical to the input port.

The ratio of r_1 to r_2 shown in Fig. 2(b) is usually in the range of less than one percent to a few percent. The more near unity the ratio, the better the coupling. However, a lower r_2/r_1 ratio requires a longer converting section to produce the 90° phase difference between waves 1 and 2 [Fig. 2(c)]. The optimum length has to be determined according to the size constraints and coupling efficiency of the particular application. The converting section can be made by electroforming techniques but is achieved easily as shown in Fig. 3 by squeezing (with a precision vise) the circular waveguide between two stainless steel blocks in proper contact with the waveguide. The technique illustrated in Fig. 3 is simple and the polarization of the output wave can be monitored as the squeeze progresses. When circular polarization is achieved at the chosen frequency (or optimized over a frequency band), then the squeeze is stopped.

We have constructed a circular polarization converter operating in the *S* band and optimized at the frequency of 2.45 GHz. The converting section, made of aluminum, is 33 cm long with an average radius of ~4.6 cm and a major-to-minor radius ratio of ~1.06. The converter is tested on the setup shown in Fig. 4. The output wave of the converter is radiated into a reflection-free environment and observed approximately 5 m away, on the axis of the output waveguide, with a rectangular horn antenna mounted on an axially rotatable base.

The radiation field at the position of the horn antenna can be generally expressed as a sum of the right- and left-hand circular polarized waves with amplitudes a_+ and a_-, respectively. Thus we write for the electric field

$$\mathbf{E} = [a_+(\mathbf{e}_x + i\mathbf{e}_y) + a_-(\mathbf{e}_x - i\mathbf{e}_y)]e^{-i\omega t}. \tag{1}$$
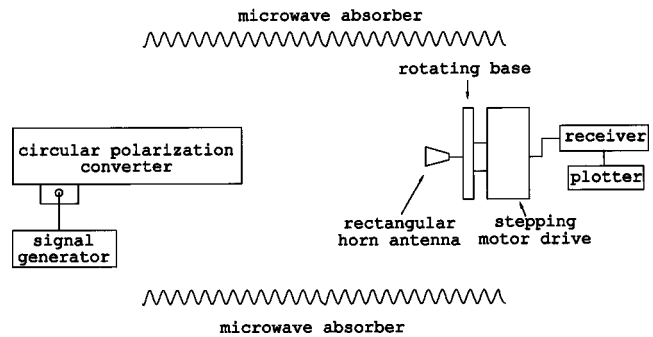

FIG. 4. The test setup for polarization measurement of the output wave from the converter.

If the polarization of the receiving horn antenna is oriented at an angle ψ with respect to the *x* axis, then the electric field strength received by the antenna is

$$E_\psi = E_x \cos(\psi) + E_y \sin(\psi) = [a_+ e^{i\psi} + a_- e^{-i\psi}]e^{-i\omega t}.$$

Hence, the received power is given by

$$P = K|E_\psi|^2 = K[|a_+|^2 + |a_-|^2 + 2\,\mathrm{Re}(a_+ a_-^* e^{2i\psi})], \tag{2}$$

where K is a proportionality constant of no significance to the polarization measurement. Clearly as we vary ψ in Eq. (2) by rotating the horn antenna, the received power will alternate between maxima and minima given, respectively, by

$$P_{\max} = K(|a_+| + |a_-|)^2 \tag{3}$$

and

$$P_{\min} = K(|a_+| - |a_-|)^2, \tag{4}$$

where $P_{\max}$ and $P_{\min}$ depend only on the amplitudes, but not the phase angles, of a_+ and a_-.

We define the polarization ratio $R(=|a_+/a_-|^2)$ as a measure of the relative power levels of the two circularly polarized components. By assuming $|a_+| > |a_-|$, we obtain from Eqs. (3) and (4),

$$R = \frac{|a_+|^2}{|a_-|^2} = \frac{[1 + (P_{\min}/P_{\max})^{1/2}]^2}{[1 - (P_{\min}/P_{\max})^{1/2}]^2}. \tag{5}$$

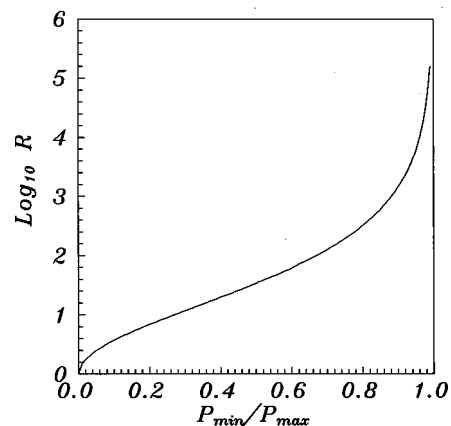A graphic representation of Eq. (5) is shown in Fig. 5.

FIG. 5. A graphic representation of the polarization ratio as a function of $P_{\min}/P_{\max}$.
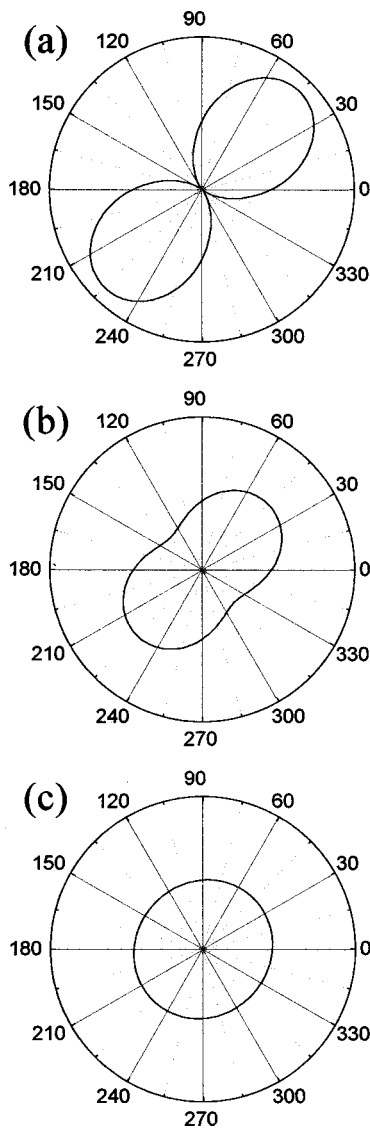
FIG. 6. Measured polarization states of the 2.45 GHz output wave emerging from the converter with (a) an unsqueezed converting section, (b) and under-squeezed converting section, and (c) an optimally squeezed converting section.

FIG. 7. Frequency response of the converter with its converting section optimized for 2.45 GHz.

In the test, the state of polarization of the converter output was monitored while the converting section was being squeezed by the method shown in Fig. 3. The power received by the horn antenna, as the rectangular horn antenna underwent a 360° rotation, was recorded in polar coordinates in Fig. 6. P_{max} and P_{min} as read from the polarization patterns in Fig. 6 can be used to infer the polarization ratio through Eq. (5). Figure 6(a) represents a linearly polarized wave ($R=1$ or $P_{min}=0$) from the output end of an unsqueezed converting section. Figure 6(b) shows an elliptically polarized wave ($R\simeq32.4$) from the output end of a half-way squeezed converting section. As the converting section was optimally squeezed, the measured polarization [Fig. 6(c)] was almost completely circular, with a polarization ratio of ~3400.

Dispersive properties of the waveguide modes are reduced as the wave frequency increases. Hence, the accumulated phase difference ($\Delta\phi$) between the two linearly polarized waves in Fig. 2(c) is, rather than a constant, a decreasing
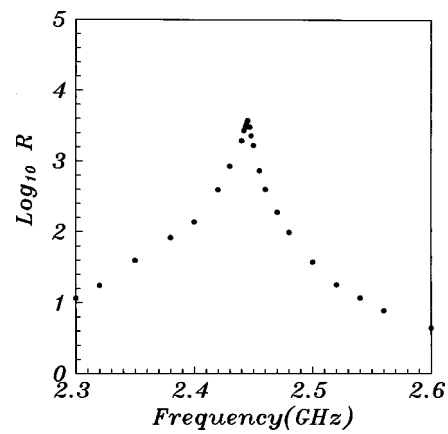
function of the wave frequency. Figure 7 shows the measured polarization ratio (in log scale) as a function of the frequency. The polarization ratio has a maximum near 2.45 GHz, the frequency of our high power source. For frequencies lower and higher than 2.45 GHz, the converting section is over and under squeezed, respectively, both resulting in a lower polarization ratio.

As shown in Fig. 7, the converter is relatively broad band for ECR applications, with a bandwidth of ~4% within which the polarization ratio exceeds 100. In the construction of the converter, the slope of the polarization ratio as a function of the frequency provides a useful test as to whether the converting section is optimally squeezed for the desired frequency. A negative slope at the desired frequency indicates under squeezing ($\Delta\phi<90°$), A positive slope indicates over squeezing ($\Delta\phi>90°$).

With a matched load placed at the output port, the converter exhibits very low return loss. As shown in Fig. 8, the return loss measured at the input port is 25 dB at 2.45 GHz and lower than 20 dB over a bandwidth of 4%. The low return loss (Fig. 8) and high polarization ratio (Fig. 7) make the device a highly efficient polarization converter. The conversion loss principally comes from the ohmic dissipation on the aluminum walls (~3% from input port to output port),
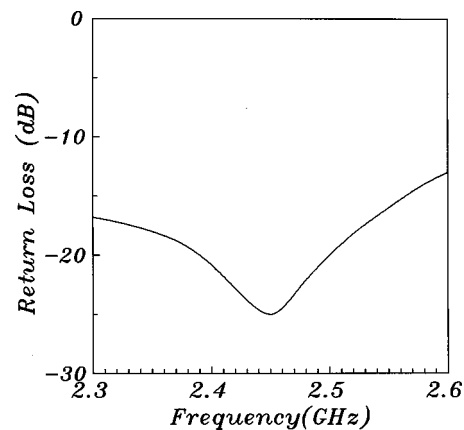

FIG. 8. Return loss measured at the input port with the output port terminated by a matched load.

which can be reduced by, for example, coating the walls with a good conducting material.

The isolation of the reflected wave can be measured by placing a short at the output port. The circularly polarized wave will be totally reflected at the short. On its return path, the reflected wave (circularly polarized at the shorted end) will convert back to a linearly polarized wave at the input end with its polarization rotated by 90° with respect to that of the incident wave (as described in Sec. II). Over a bandwidth of 4% centered at 2.45 GHz, powers of the reflected wave as measured at the reflected-wave port and input port (Fig. 1) are, respectively, 93% and less than 1% of the incident power, the rest being dissipated on the converter walls. Thus, the converter provides a 20 dB rejection of the reflected wave over a bandwidth of ~4%. This, together with its simple structure, permits high power operation without the use of an isolator for the protection of the source.

ACKNOWLEDGMENTS

[1] J. Asmussen, *Handbook of Plasma Processing Technology*, edited by S. M. Rossnagel, J. J. Cuomo, and W. D. Westwood (Noyes, New Jersey, 1990), Chap. 11.

[2] O. A. Popov, *Physics of Thin Film*, edited by M. H. Francombe, and J. L. Vossen (Academic, New York, 1994), pp. 121–233.

[3] J. E. Stevens, *High Density Plasma Sources*, edited by O. A. Popov (Noyes, New Jersey, 1995), Chap. 7.

[4] M. A. Lieberman and R. A. Gottscho, *Physics of Thin Film*, edited by M. H. Francome and J. L. Vossen (Academic, New York, 1994), pp. 25–40.

[5] M. A. Lieberman and A. J. Lichtenberg, *Principles of Plasma Discharges and Materials Processing* (Wiley, New York, 1994), Chap. 13.

[6] J. Musil and F. Zacek, Phys. Plasmas **13**, 471 (1971).

[7] Y. Sakamoto, Jpn. J. Appl. Phys. **16**, 1993 (1977).

[8] O. A. Popov and H. Waldron, J. Vac. Sci. Technol. A **7**, 914 (1989).

[9] J. E. Stevens, J. L. Cecchi, Y. C. Huang, and R. L. Jarecki, J. Vac. Sci. Technol. A **9**, 696 (1991).

[10] O. A. Popov, S. Y. Shapoval, and M. D. Yoder, Jr., Plasma Sources Sci. Technol. **1**, 7 (1992).

[11] O. A. Popov, J. Vac. Sci. Technol. A **8**, 2909 (1990).

[12] S. Samukawa, J. Vac. Sci. Technol. A **11**, 2572 (1993).

[13] M. Matsuoka and K. Ono, J. Vac. Sci. Technol. A **9**, 691 (1991).

[14] J. Asmussen, T. A. Grotjohn, P. U. Mak, and M. A. Perrin, IEEE Trans. Plasma Sci. **25**, 1196 (1997).

[15] A. Vegas, M. A. G. Calderon, and E. G. Bustamante, Plasma Phys. Controlled Fusion **26**, 1579 (1984).

[16] T. Ege and P. McAndrew, Electron. Lett. **21**, 1166 (1985).

[17] N. C. Albertsen and P. Skov-Madsen, IEEE Trans. Microwave Theory Tech. **31**, 654 (1983).

[18] J. Bornemann and V. A. Labay, IEEE Trans. Microwave Theory Tech. **43**, 1782 (1995).

[19] S. F. Adam, *Microwave Theory and Application* (Prentice–Hall, Englewood Cliffs, NJ, 1969), pp. 62 and 63.

[20] L. R. Barnett, L. H. Chang, H. Y. Chen, K. R. Chu, W. K. Lau, and C. C. Tu, Phys. Rev. Lett. **63**, 1062 (1989).

[21] K. R. Chu, L. R. Barnett, W. K. Lau, L. H. Chang, and H. Y. Chen, IEEE Trans. Electron Devices **37**, 1557 (1990).